JOURNAL OF MATERIALS SCIENCE **40** (2005) 5581–5589

Effect of sintering schedule on grain size of oxide ceramics

KAREL MACA*, SARKA SIMONIKOVA
Department of Ceramics, Brno University of Technology, Technica 2, 616 69 Brno, Czech Republic
E-mail: maca@fme.vutbr.cz

Published online: 25 August 2005

The sintering and grain size of sub-micrometric CeO_2 and ZrO_2 + 3 mol%Y_2O_3 prepared by injection moulding and cold isostatic pressing were studied. Using combinations of the ceramic powders used and shaping methods, three types of bodies were prepared that were characteristic by their own green body microstructure. Their sintering behaviour was described with the aid of high-temperature dilatometry. Each type of specimen was then sintered to two levels of final density (higher than 98% t.d.), for each density always via two or three different firing modes differing in temperature and holding time. In the ZrO_2 specimen it was verified statistically that the final grain size was the same irrespective of whether the given final density was obtained by sintering for a longer period at a lower temperature or for a shorter period at a higher temperature. This finding did not hold for the injection moulded CeO_2 cylinders, which contained cavities in the order of millimetre. When these defects in the structure of CeO_2 ceramic were removed, it was verified statistically also for this material that the final grain size was a function of the density obtained and not the temperature cycle with which this density was obtained.

1. Introduction

The properties of ceramic materials are greatly affected by their microstructure, i.e. their density, distribution of grain size and pores, and other defects. For example, the grain size influences the mechanical [1, 2], tribological [3], electrical [4], biological [5], and optical properties [6]. Decreasing grain size leads to increased strength [1], hardness [2], electric conductance along grain boundaries [4], resistance to mechanical [3] and biological wear [5], and transparency [6] of ceramic materials.

The sintering process of advanced ceramic materials is most often aimed at obtaining a material of high relative density, homogeneous microstructure, and small grains. It is well known that sintering behaviour and final grain size are affected in particular by the particle size of starting ceramic material, the degree of its agglomeration and also by the microstructure of green body, which in addition to powder material is also determined by the shaping technology used [7–9]. However, no consistent opinion can be found in the literature as to whether the final grain size of a concrete body of a given density can be influenced by the choice of sintering schedule. There are papers claiming that an appropriate choice of the sintering schedule can result in fine-grain microstructures [10–14] while others, on the contrary, claim that obtaining a given density clearly determines the specimen grain size (with the exception of additional grain growth after reaching the ultimate sample density) [15–19].

It has been the aim of the present paper to assess the effect of sintering schedule on the microstructure of CeO_2 and yttria-stabilized ZrO_2, which are advanced and widely used materials employed in structural, biological and electroceramic applications. The paper should make it clear whether from the viewpoint of final microstructure it is important what temperature schedule we choose in order to obtain the final density. It was examined whether sintering for a shorter period at a higher temperature results in a different final grain size than sintering for a longer period at a lower temperature while the same final density is obtained.

2. Experimental

2.1. Materials

The following types of ceramic powder material were used for the preparation of ceramic specimens:

- ZrO_2 stabilized with 3 mol% Y_2O_3, type TZ-3YS (Tosoh, Japan). The mean particle size measured by laser diffraction was 0.56 μm, the crystal size given by the manufacturer was 0.036 μm. This zirconia powder was used for injection moulding.

*Author to whom all correspondence should be addressed.
0022-2461
DOI: 10.1007/s10853-005-1332-1

- granulated ZrO_2 stabilized with 3 mol% Y_2O_3, type TZ-3YB (Tosoh, Japan). This powder contained granules of 20–50 μm in size, the crystallite size given by the manufacturer was 0.027 μm. This zirconia powder was used for cold isostatic pressing.
- CeO_2 powder (Guangzhou Zhuijang Refinery, China). The mean particle size established by laser diffraction was 0.37 μm.

2.2. Specimen preparation prior to sintering

The above ceramic powder materials were shaped into cylinders (dia 5.9 mm, height 60 mm) via injection moulding (Allrounder injection press, Germany) and disks (dia 30 mm, height 5 mm) via cold isostatic pressing (Autoclave Engineering, Inc., USA). Injection moulded specimens were then debinded and presintered at 800°C/1 h. Isostatically pressed disks were cut and ground into prisms. Three kinds of specimen were prepared:

- injection moulded ZrO_2 – Z/IM in the following — in the form of cylinders
- cold isostatically pressed ZrO_2 – Z/CIP in the following — in the form of prisms
- injection moulded CeO_2 – C/IM in the following — in the form of cylinders and prisms

2.3. Sintering of ceramic specimens

The specimens were first sintered in a high-temperature dilatometer (L70/1700, Linseis, Germany) with vertical specimen orientation. The specimen was heated in a graphite furnace working under slight nitrogen overpressure. The measuring system made of Al_2O_3 and specimen were placed in a closed Al_2O_3 tube with air atmosphere. The schematic diagram of experiment layout is given in Fig. 1. The dimensions of the specimens designed for sintering in high-temperature dilatometer were: dia 5.9 mm, height 15 mm (cylinders) and 3 × 4 × 15 mm (prisms). The front surfaces of specimens were ground such that they were planparallel.

For each type of specimen, 3 different sintering temperatures were chosen such that final relative densities of 95% t.d. and higher were obtained. For the C/IM and Z/CIP specimens these temperatures were 1400, 1450 and 1500°C while for the Z/IM specimens they were 1450, 1500 and 1530°C. The temperature was being increased at a rate of 10°C/min up to a temperature of 800°C and then at a rate of 5°C/min up to the final temperature, at which the isothermal holding time followed (2 h for the C/IM and Z/CIP specimens, and 3 h for the Z/IM specimens). Cooling proceeded at a rate of 25°C/min down to 1000°C, after which the specimen was left to cool freely. After sintering, the bulk density of specimens was established on the basis of Archimedes' principle. Based on the bulk density, the relative density of specimens ($\rho_{rel}(\%)$) was calculated, using theoretical densities of 6.08 g/cm^3 for ZrO_2 + 3 mol% Y_2O_3, and 7.132 g/cm^3 for CeO_2.

The output data, which were continually recorded by the dilatometer, were converted from the dependence

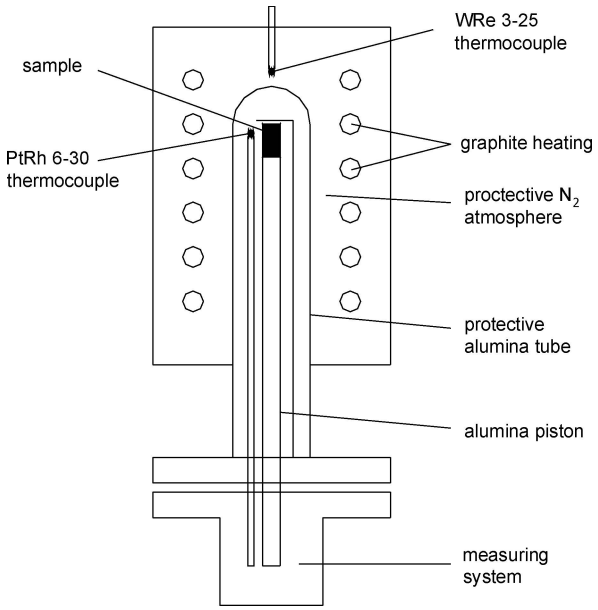

Figure 1 Schematic diagram of high-temperature dilatometer.

of specimen shrinkage on time and temperature $\varepsilon(t,T)$ to the dependence of relative density on time and temperature $\rho_{rel}(t,T)$ by relation (1):

$$\rho_{rel}(t,T) = \rho_{relf} \cdot \frac{100+\varepsilon_l}{100+\varepsilon(t,T)} \cdot \frac{100+k_a\cdot\varepsilon_l}{100+k_a\cdot\varepsilon(t,T)} \cdot \frac{100+k_b\cdot\varepsilon_l}{100+k_b\cdot\varepsilon(t,T)}, \quad (1)$$

where ρ_{relf} (%) is the final relative density of specimen ε_l (%) is the final longitudinal shrinkage of specimen k_a and k_b (−) are the anisotropy coefficients defined by the relations

$$k_a = \frac{\varepsilon_a}{\varepsilon_l}, \quad k_b = \frac{\varepsilon_b}{\varepsilon_l}, \quad (2)$$

where ε_a and ε_b (%) are the final transverse shrinkages of specimen established from micrometer measurements of the transverse dimensions of specimen.

Dependence relations $\rho_{rel}(t,T)$ were used to establish concrete firing schedules leading to identical densities of specimens sintered at different temperatures and holding times. Firing in these schedules was then performed in a standard resistance (superkanthal) furnace (K 1700/1, Heraeus, Germany). The dimensions of specimens designed for sintering in a conventional resistor furnace were: dia 5.9 mm, height 8 mm (cylinders) and 3 × 4 × 4 mm (prisms). The temperature increase to the sintering temperature was the same as for sintering in the high-temperature dilatometer: 10°C/min up to 800°C, 5°C/min up to the sintering temperature, and then the prescribed holding time was followed by cooling at a rate of 25°C/min.

2.4. Microstructure of sintered specimens

After sintering the final specimen densities were measured using the method described above. The specimens were then cut, polished and thermally etched

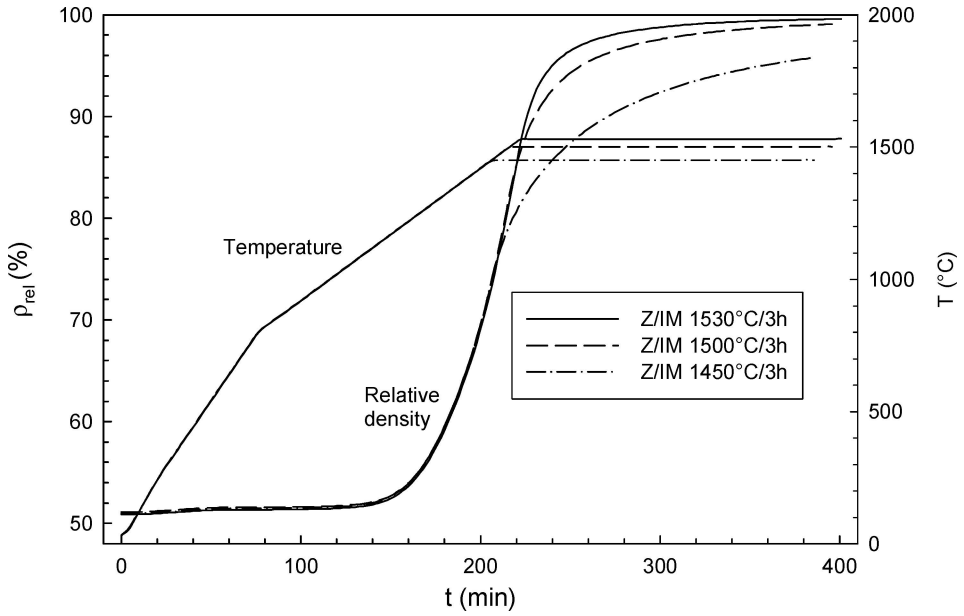

Figure 2 Dependence of relative density of injection moulded ZrO_2 and temperature on time.

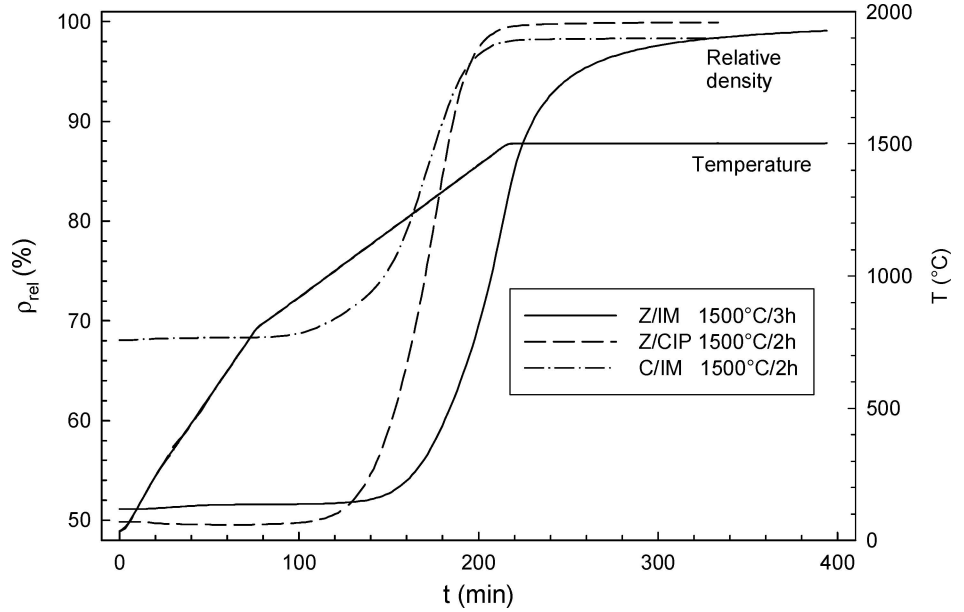

Figure 3 Comparison of sintering curves (1500°C) of all the three types of material used.

(1400°C/5 min) to make the grain boundaries more pronounced. The microstructure of specimens was studied using scanning electron microscopy (SEM) (Philips XL30, the Netherlands). To make the specimens conductive, they were coated with a layer of gold and palladium. The mean grain size (D) of sintered ceramic materials was established via the linear intercept method. For each specimen, 15 line segments were evaluated. Used as a basis for grain size evaluation were pictures obtained on the SEM.

3. Results and discussion

3.1. Prediction of sintering schedules leading to identical densities

The data obtained from specimen sintering in the high-temperature dilatometer were used (on the basis of procedure given in the experimental section) to fully describe the development of relative specimen density in dependence on temperature and time. For illustration, Fig. 2 gives the sintering curves of injection moulded ZrO_2 (Z/IM). It is obvious from the Figure that the density obtained increased with increasing holding temperature, and also evident is the good agreement of all the three sintering curves up to a temperature of 1450°C. This agreement indicates a high reproducibility of the measurement.

Fig. 3 offers a comparison of the sintering curves for all the three types of specimen sintered at a temperature of 1500°C. It is evident from the comparison that the material that sintered best (i.e. at the lowest temperatures and up to the highest final relative densities) was Z/CIP, in spite of having the lowest starting density of all the materials used. This material was the only one that had not been pre-sintered to 800°C but, as can be seen from its density development in Fig. 3, not even

pre-sintering to 800°C would have increased its green density. These results are in agreement with the opinion that there is no direct proportion between the density prior to sintering and the kinetics of sintering since the total volume of pores in green body is less important than their size distribution, in particular the elimination of large pores [8, 9].

Fig. 4a–c give details of the curves of the final sintering stage (the closed porosity phase). It is obvious from these graphs that for each type of specimen two values of final density were chosen that had been obtained by at least two different firing modes. From the dependence $\rho_{rel} = f(t,T)$ it was then established what holding time at the given temperature was necessary to obtain this density. A survey of the selected values of final density and the temperature cycles that led to them is given in Table I.

3.2. Sintering according to the chosen temperature cycles

Table II gives the final relative density values obtained after sintering according to the temperature cycles chosen. For reasons of time and economy these experiments were not carried out in a dilatometer but in a standard resistance furnace.

The results given in Table II make it evident that specimens sintered in the resistance furnace reached higher final densities than had been assumed from analyses of dilatometric curves. To eliminate the effect of incorrectly determined temperature in one (or both) sintering furnace(s), the temperature was checked by installing another thermocouple, which was placed in immediate vicinity of the specimen, successively in the dilatometer and in a conventional furnace. It was found from this measurement that the two temperatures differed at individual sintering temperatures by a maximum of 5°C, which is a difference that cannot have caused such marked differences in the density. The reason for the difference in final densities in the dilatometer and in the conventional furnace is not known yet; one possible reason might consist in atmospheric pressure. While the gas in a conventional furnace flows freely around the specimen, the specimen in the dilatometer is placed in the top of a closed alumina tube, which insulates it from graphite heating (see Fig. 1). In view of the high temperature in this area, and the impossibility of free air convection around the specimen, the pressure of atmosphere close to the specimen might exceed one atmosphere. The pressure was checked in the area between the closed alumina tube (which is vacuum sealed) and the measuring system (which is not vacuum sealed) and at this vertical level the pressure was 1.05 atm. Increased pressure around the sample would have an adverse effect on sintering, in particular in the closed porosity phase, when molecules of the gas atmosphere must diffuse along grain boundaries from the closed pores. This adverse effect on specimen sintering in a dilatometer was established for the first time in the course of the present work and it will be further examined.

As can be seen from the results given in Table II, the densities obtained by sintering in the conventional furnace did differ from the densities obtained in the

TABLE I Selected values of final density and the temperature cycles that led to them

		Sintering temperature (°C)			
Specimen marking	ρ_{relf} (%)	1400°C	1450°C	1500°C	1530°C
Z/IM	95.6		1450°C/177′	1500°C/45′	1530°C/20′
	99.0			1500°C/163′	1530°C/90′
Z/CIP	99.5	1400°C/35′	1450°C/8′	1500°C/1′	
	99.8	1400°C/94′	1450°C/43′	1500°C/34′	
C/IM	97.6	1400°C/110′	1450°C/3′	1458°C/0′	
	98.1		1450°C/100′	1500°C/5′	

TABLE II Final relative densities and grain size obtained after sintering according to the temperature cycles chosen

Specimen marking	Assumed density (%)	Sintering (°C/min)	ρ_{relf} (%)	D (μm)	s (μm)	n (−)
Z/IM-A	95.6	1450/177	99.0	0.254	0.032	15
Z/IM-B		1500/45	98.9	0.263	0.024	15
Z/IM-C	99.0	1530/20	99.1	0.266	0.026	15
Z/IM-D		1500/163	99.8	0.361	0.059	15
Z/IM-E		1530/90	99.8	0.350	0.043	15
Z/CIP-F	99.5	1400/35	99.8	0.166	0.015	15
Z/CIP-G		1450/8	99.6	0.170	0.014	15
Z/CIP-H		1500/1	99.8	0.177	0.011	15
Z/CIP-I	99.8	1400/94	99.9	0.194	0.015	15
Z/CIP-J		1450/43	99.9	0.194	0.024	15
Z/CIP-K		1500/34	100.0	0.213	0.021	15
C/IM-L	97.6	1400/110	98.3	3.114	0.316	15
C/IM-M		1450/3	98.3	2.581	0.199	15
C/IM-N	98.1	1458/0	98.3	3.620	0.386	15
C/IM-O		1450/100	98.5	8.669	1.158	15
C/IM-P		1500/5	98.4	8.003	0.616	15

s — standard deviation, n — number of measurements

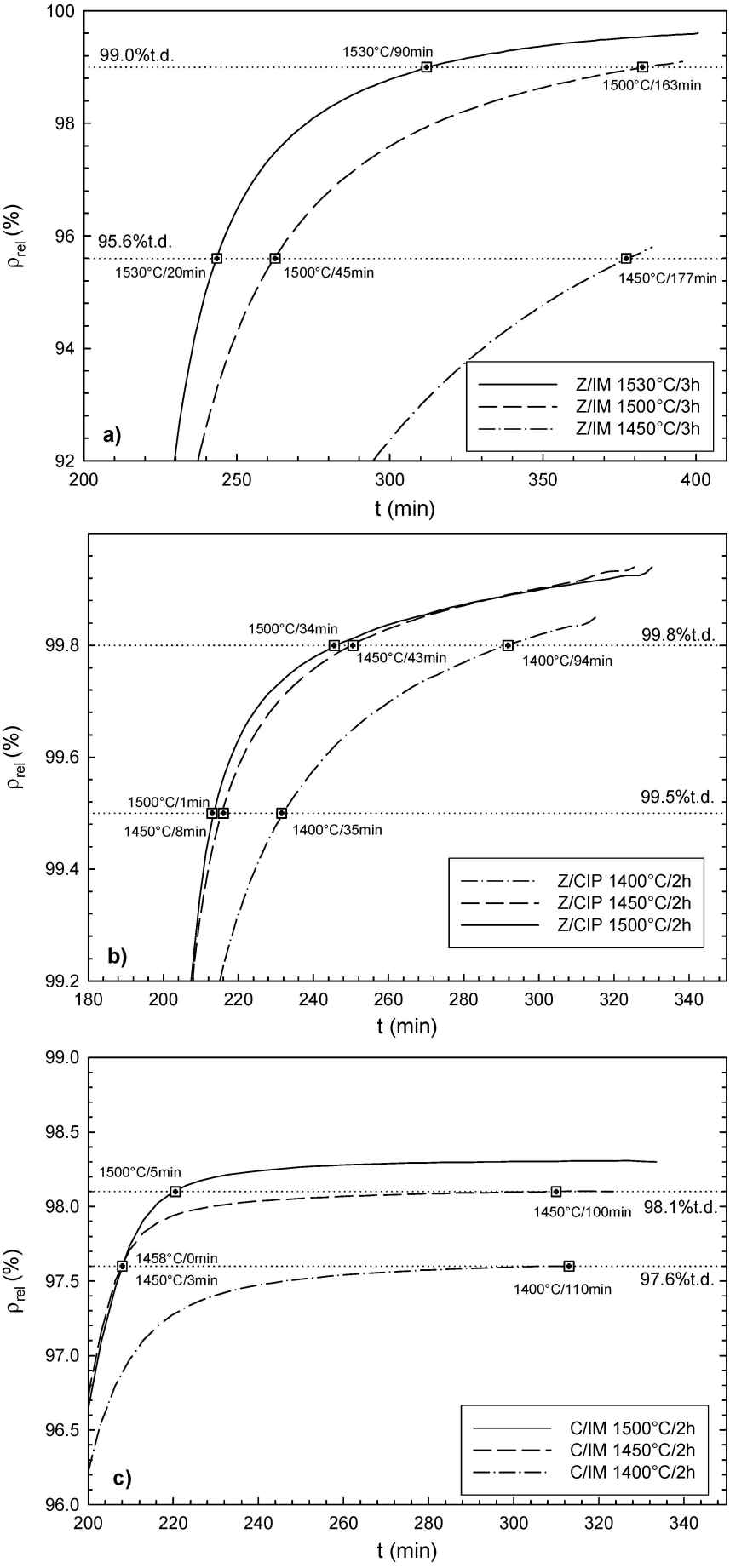

Figure 4 Details of sintering curves in the final stage sintering: (a) injection moulded ZrO_2 cylinders, (b) cold isostatically pressed ZrO_2 prisms, and (c) injection moulded CeO_2 cylinders.

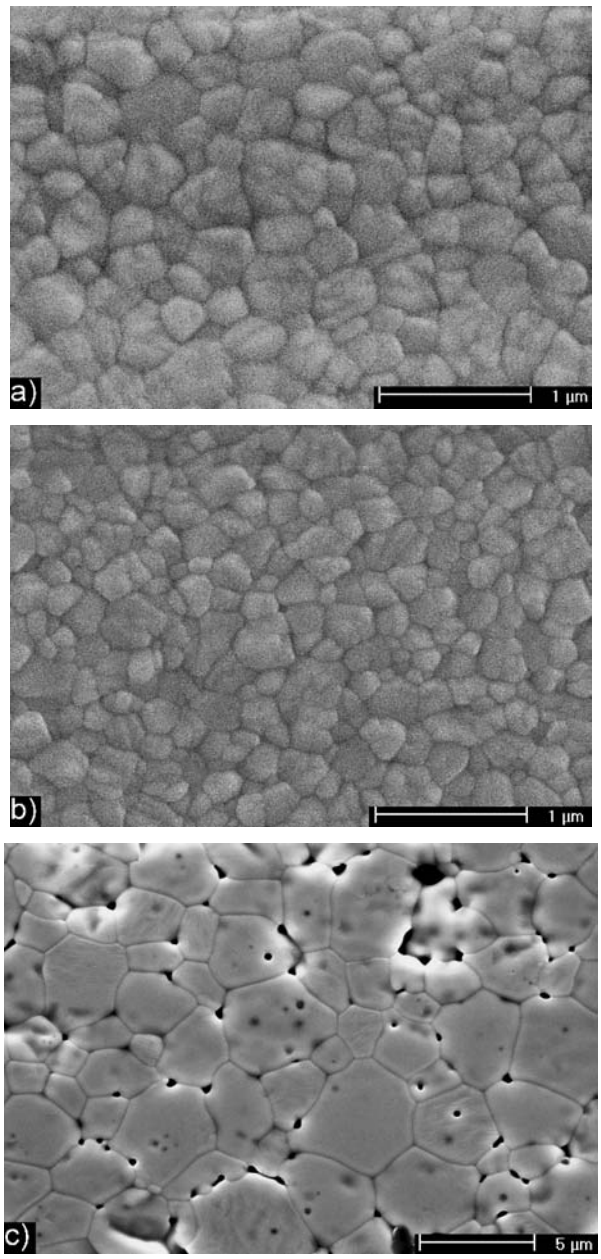

Figure 5 Microstructure of thermally etched sections of sintered ceramics: (a) Z/IM - B, sintered at 1500°C/45 min, (b) Z/CIP - H, sintered at 1500°C/1 min, and (c) C/IM - L (cylinder), sintered at 1400°C/110 min.

dilatometer but the firing cycles chosen led to comparable densities, which satisfied the objectives of the present work; only the range of final relative densities was shifted from the 95–100% interval (see Fig. 4) to densities of 98–100% (see Table II).

3.3. Microstructure of sintered specimens

Fig. 5a–c give the typical microstructures of selected thermally etched sections of sintered specimens. In zirconia specimens (Fig. 5a, and b) no pores could be seen, which corresponded to the measured final relative densities of 99% and higher. The grain size ranged in the order of tenths of micrometer.

The microstructure of injection moulded CeO_2 specimens was different. It is obvious from Fig. 5c that the ceramic material contained a large amount of pores, mostly on the grain boundaries. This high porosity was reflected in the lower final relative density (see Table II). The pore size was up to the order of micrometer but, in addition, there were also cavities in the microstructure, in the order of millimetre. The origin of these cavities can probably be sought in the injection moulding process (air being mixed into thermoplastic mixture). As can be seen from Fig. 3, the C/IM specimen sintered at lower temperatures than Z/IM did, but at the holding time its relative density stopped at a value of ca. 98% and did not increase any more. Similar behaviour has been described for sub-micrometric Al_2O_3 [9]. In the paper, the author has shown that remaining porosity is in such a case the "responsibility" of the large isolated pores, which in principle are defects originating in the course of shaping the bodies.

3.4. Grain size of sintered specimens

The grain size of sintered specimens established by the linear intersection method is given in Table II, and graphically represented in Fig. 6a–c. It is evident from Table II and Fig. 6a–c that specimens sintered to the same (or very similar) density were (within the standard deviation) of the same grain size, with the only exception of the C/IM specimens sintered to 98.3% t.d., for which the $D \pm s$ intervals did not overlap. The sets of grain sizes measured were put to the non-parametric two-selection Wilcoxon test, which tested the hypothesis that the grain-size distribution functions of two different samples are identical. For all the sets with the same final density this hypothesis could not at significance level $\alpha = 0.05$ be disproved, with the exception of the CeO_2 cylinders sintered to 98.3% t.d. (C/IM – L, M, N), whose grain sizes were different with a probability of as much as 99%.

3.5. Sintering of CeO_2 prisms

The difference in the grain size of CeO_2 cylinders sintered to the same final density using different temperature cycles need not have been a property of this material and could have been caused by the great inhomogeneity of these specimens. The final density of these specimens was, on the one hand, a function of the sintering schedule and, on the other hand, also a function of the presence of random volume of cavities in the given specimen.

To eliminate the effect of random defects in the structure of CeO_2 cylinders, additional experiments were carried out via sintering injection moulded CeO_2 prisms that, due to the different method of filling the mould in injection moulding, did not contain these defects. These experiments were only made in the dilatometer, with the specimen being first sintered at a holding time of 40 min at a temperature of 1500°C and reaching a final relative density of 99.5%. The same material was then sintered in the "rate-controlled sintering" (RCS) mode so as to also obtain a final density of 99.5%. In the RSC method the heating of specimen is controlled such that the specimen density increases according to a preset time schedule. The authors of this method have declared that if the rate of specimen

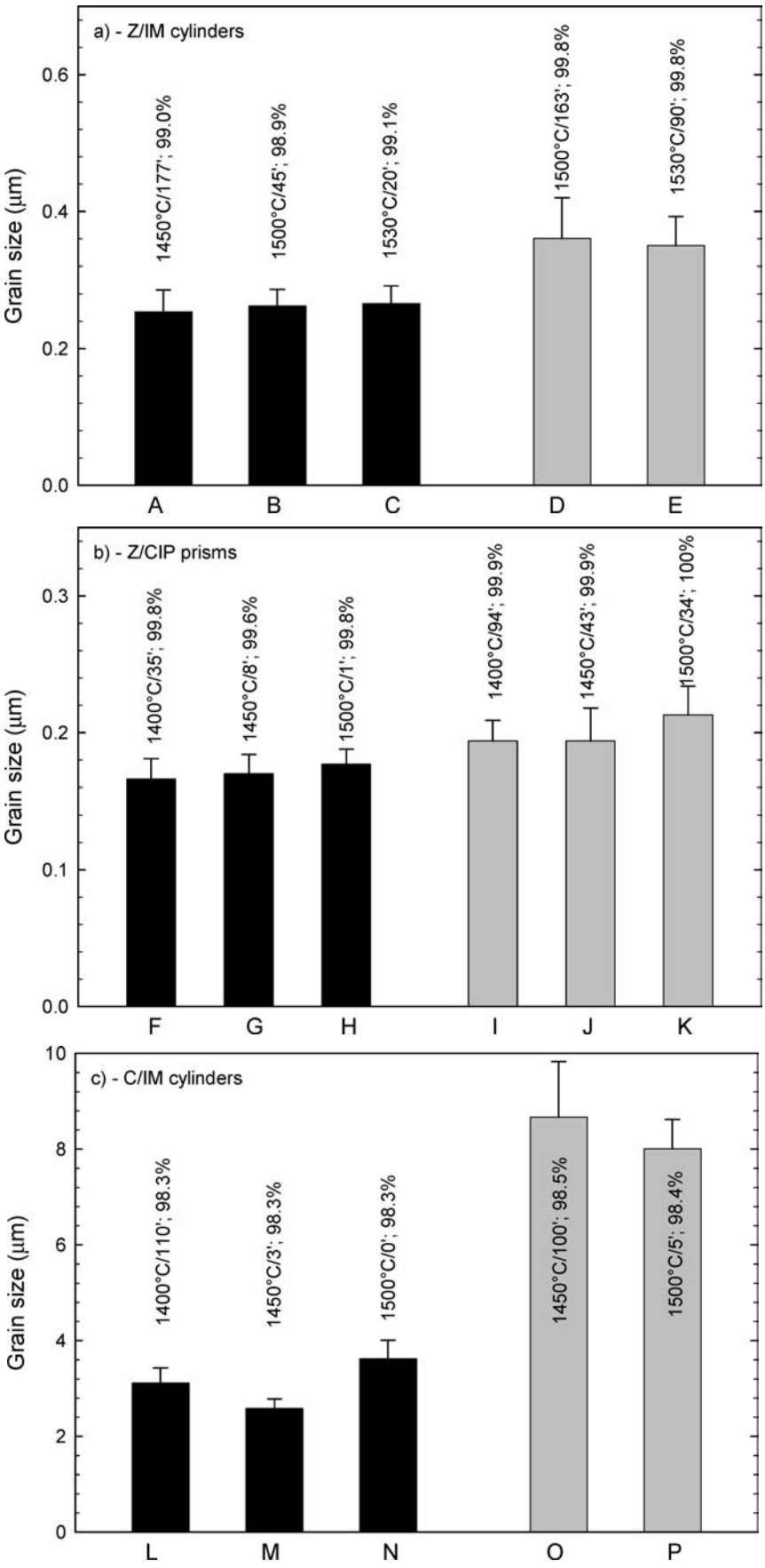

Figure 6 Mean grain size of specimens sintered with different temperature modes: (a) injection moulded ZrO_2 cylinders, (b) cold isostatically pressed ZrO_2 prisms, and (c) injection moulded CeO_2 cylinders.

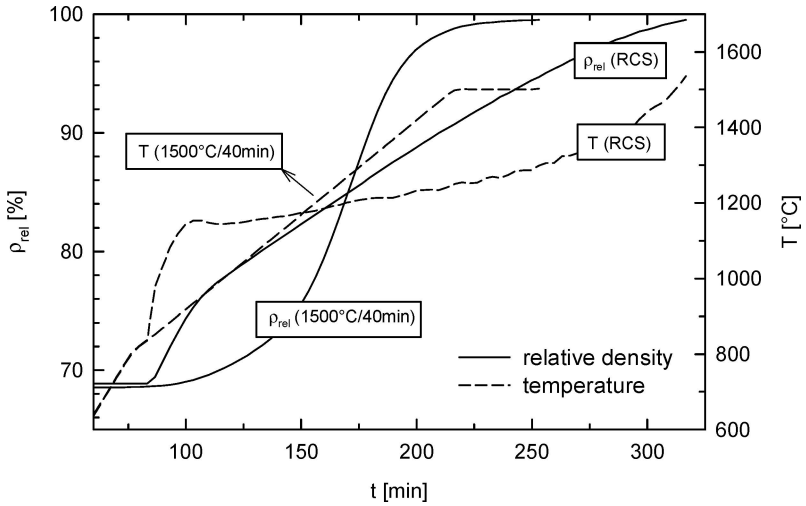

Figure 7 Time-dependence of relative density and temperature of injection moulded CeO_2 prisms while sintering at 1500°C/40 min, and by the RCS method.

densification is sufficiently low in the open porosity phase, the result is a material with finer grains than in the case with the more frequently applied method of temperature-controlled sintering (TCS = heating at a constant rate and holding time at the sintering temperature) [10, 11]. In the present work the procedure published in the patent for the RCS method [10] was strictly observed, after which the specimen also had a final relative density of 99.5%. The dependence of the density of specimens and their temperatures on time for a CeO_2 prism sintered with both the RCS and the TCS method is given in the plot in Fig. 7. It is obvious from this plot that identical final densities were obtained with completely different temperature cycles.

Fig. 8a and b show the microstructure of sintered and thermally etched sections through these specimens. As already indicated by the density measurement, the specimens were very well sintered, the dark spots in microphotographs are not pores but ZrO_2 inclusions originating from the milling process. Table III gives the mean grain sizes of both specimens, established by the linear intercept method. It can be seen from the Table that specimens sintered to the same final density using quite different temperature modes had (within the measurement error) the same final grain size, which was also confirmed at significance level $\alpha = 0.05$ by the two-selection Wilcoxon test.

These additional experiments showed that it was also true for CeO_2 that essential for the grain size was the density obtained and not the sintering mode used to obtain this density. It should be stressed, however, that the above hypothesis does not hold for a given ceramic material in general but directly for a given specimen characterized by the microstructure of ceramic green body, which is the result of the given moulding method, and that in the present work this hypothesis was verified for densities close to theoretical density.

TABLE III Final relative densities and mean grain size of injection moulded CeO_2 prisms

Specimen marking	Sintering (°C/min)	ρ_{relf} (%)	D (μm)	s (μm)	n (−)
C/IM prism	1500/ 40	99.52	2.76	0.24	15
C/IM prism	RCS	99.51	2.96	0.33	15

s-standard deviation, n-number of measurements.

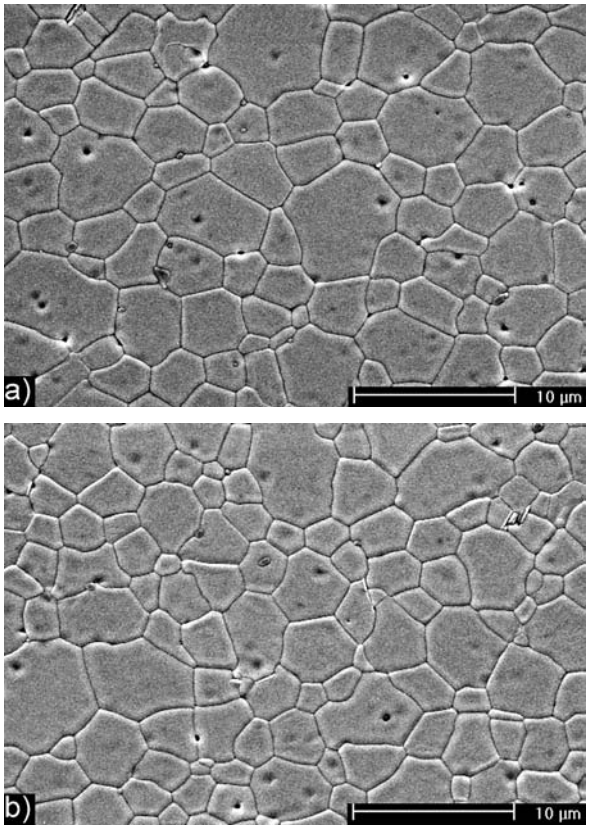

Figure 8 Microstructure of injection moulded CeO_2 prisms: (a) sintered at 1500°C/40 min, and (b) sintered by the RCS method.

The results presented in this work are not only of theoretical importance but also of practical importance: in industrial practice they enable technologists to freely choose a sintering schedule in dependence on the required savings in time, power or depreciation.

4. Conclusion

Via controlled sintering of injection moulded ceramic materials CeO_2 and ZrO_2 + 3 mol% Y_2O_3 and cold

isostatically pressed ZrO_2 + 3 mol Y_2O_3 the same final specimen densities were obtained by different sintering schedules (a longer holding time at a lower temperature or a shorter holding time at a higher temperature in isothermal sintering or in rate-controlled sintering). While examining the microstructure of sintered specimens it was proved statistically that the choice of sintering schedule did not have any effect on the grain size of sintered material, which means that for a given specimen (characterized by the microstructure of ceramic green body, i.e. by the distribution of particle and pore sizes) the grain size is a function of specimen density irrespective of the temperature mode with which this density has been obtained.

Acknowledgments

This work was supported by the Czech Ministry of Education by the Grant No. VZ CEZ: J22/98. The authors express their thanks also to Dr. D. Janova for carrying out the SEM analyses.

References

1. A. KRELL and P. BLANK, *J. Eur. Ceram. Soc.* **16** (1996) 1189.
2. *Idem.*, *J. Am. Ceram. Soc.* **78** (1995) 1118.
3. Y. J. HE, L. WINNUBST, A. J. BURGGRAAF, H. VERWEIJ, P. G. T. VAN DER VARST and B. DE WITH, *ibid.* **79** (1996) 3090.
4. G. XU, Y.-W. ZHANG, CH.-S. LIAO and CH.-H. YAN, *Solid State Ions.* **166** (2004) 391.
5. S. LAWSON, *J. Eur. Ceram. Soc.* **15** (1995) 485.
6. R. APETZ and M. P. B. VAN BRUGGEN, *J. Am. Ceram. Soc.* **86** (2003) 480.
7. F. W. DYNYS and J. W. HALLORAN, *ibid.* **66** (1984) 596.
8. A. ROSEN and H. K. BOWEN, *ibid.* **71** (1998) 970.
9. J. ZHENG and J. S. REED, *ibid.* **72** (1989) 810.
10. H. PALMOUR III. and M. L. HUCKABEE, Process for sintering finely derived particulates and resulting ceramics products. U.S. Patent 3900542, August 19, 1975.
11. M. L. HUCKABEE and H. PALMOUR III., *Am. Ceram. Soc. Bull.* **51** (1976) 574.
12. G. AGARWAL, R. F. SPEYER and W. S. HACKENBERGER, *J. Mater. Res.* **11** (1996) 671.
13. S.-Y. LEE, *Ceram. Intern.* **30** (2004) 579.
14. K. MACA, H. HADRABA and J. CIHLAR, in Ceramics — Processing, Reliability, Tribology and Wear, edited by G. Mueller (Wiley-VCH, Weinheim, 2000) p. 161
15. R. L. COBLE and T. G. GUPTA, in Sintering and Related Phenomena, edited by G. C. Kuczynski, N. A. Hooton and C. F. Gibbon (Gordon and Breach, New York, 1967) p. 423.
16. T. G. GUPTA, *J. Am. Ceram. Soc.* **55** (1972) 276.
17. H. SU and D. L. JOHNSON, *ibid.* **79** (1996) 3211.
18. J. WANG and R. RAJ, *ibid.* **73** (1996) 1172.
19. Z. XIE, J. YANG and Y. HUANG, *Mater. Lett.* **37** (1998) 215.
20. M. TRUNEC, P. DOBSAK and J. CIHLAR, *J. Eur. Ceram. Soc.* **20** (2000) 859.

Received 25 August 2004
and accepted 1 April 2005